

Reach of an inclined cantilever with a tip load

P. SINGH, V. G. A. GOSS

School of Engineering, London South Bank University, London SE1 0AA, UK,

e-mails: singhp9@lsbu.ac.uk, gossqa@lsbu.ac.uk

WE INVESTIGATE THE PROBLEM OF DETERMINING THE REACH of an inclined cantilever for a given point load suspended from its tip. Two situations are considered. Firstly, we find the maximum reach of the cantilever by varying its angle of inclination. Secondly, we find the reach of the cantilever subject to the condition that its tip is at some specified height, above or below, the level of the clamped end. In the second case, the reach of the cantilever is maximised by shortening its physical length whilst keeping the physical load and physical height of load deployment constant. All of our solutions representing various reaches of an inclined cantilever for a given point load suspended from its tip are shown to be stable to the snap-back instability.

Key words: clamped-free, inclined, point load, reach, snap-back instability, cantilever.

Copyright © 2019 by IPPT PAN, Warszawa

1. Introduction

LARGE DEFLECTIONS OF CANTILEVERS UNDER VARIOUS TIP LOADS has been the subject of research by many authors such as BISSHOPP and DRUCKER [1], WANG [2], NAVAEE and ELLING [3, 4] and BATISTA [5].

Recently, much attention has been devoted to the reach of an inclined cantilever with a load suspended from its tip. Wang investigated the problem of determining the angle of inclination and the longest reach of the cantilever deploying a load suspended from its tip to the same level as its clamped end [6]. That problem was solved by numerical integration. Noticing that large loads caused the cantilever to become highly deflected and the reach to become relatively short, Wang had the idea of increasing, or maximising, the reach of the cantilever by shortening its length. Numerical methods were used to demonstrate that idea. BATISTA presented an analytical approach to maximising the reach, also by shortening the length of the cantilever [7]. That approach applied calculus to the exact solutions, in terms of Jacobi elliptic functions, representing the equilibrium configurations of the inclined cantilever with a tip load. PLAUT and VIRGIN investigated the problem of determining the furthest reach of a cantilever with a load suspended from its tip [8]. In their investigation, which was experimental and numerical, the restriction that the tip load is to be deployed

to the same level as the clamped end was removed. ARMANINI *et al.* also analysed similar problems of extremal reach of a clamped-free elastic rod with a tip load in the context of the performance and design of a robot's arm for targeted reaching [9]. Their results were mainly obtained through numerical methods and corroborated experimentally.

The problems investigated in this paper, and in the references cited in the previous two paragraphs, have application in fields such as: robotics where rod-like sensors are used to navigate environments [9, 10]; nanoscience where cantilever sensors are utilised as scanning probes [11]; and disaster relief, medical aid, and fruit harvesting as continuum manipulators [12].

In this paper we first investigate the problem of determining the angle of inclination that produces the maximum reach of a cantilever for a given point load suspended from its tip. Secondly, we find the reach of the cantilever for a given point load suspended from its tip subject to the condition that the tip of the cantilever must be at some specified height, above or below, the level of the clamped end. That reach of the cantilever is then maximised by shortening its physical length whilst keeping the physical load and physical height of load deployment constant. We emphasise the importance of working in physical (dimensional) units when discussing maximising the reach by shortening the length of the cantilever as it makes no sense to shorten the length of a non-dimensional cantilever which is always normalised to one.

2. Mathematical model and exact solutions

Upper case letters refer to physical (dimensional) quantities and lower case letters refer to non-dimensional quantities. Angles are the exception to that rule, and always denoted by lower case Greek letters. Therefore, for the sake of brevity and to avoid excessive use of the words 'physical' and 'non-dimensional', we simply use the appropriate lower case or upper case letter when referring to a quantity. The case will indicate whether it is physical or non-dimensional. For example, L is a physical length and p is a non-dimensional load.

Consider a cantilever, modeled as a straight, inextensible and unsharable elastic rod, inclined at an angle α to the X -axis. The length of the cantilever is L . It is clamped at the origin and free at the other end where a point load P is suspended from its tip. The cantilever is parameterised by its arc length, $0 \leq S \leq L$ with $S = 0$ at the origin and $S = L$ at the free end or tip. The angle the tangent at any point $(X(S), Y(S))$ on the deflected cantilever makes with the X -axis is given by $\theta(S)$, see Fig. 1.

The ordinary differential equations describing the cantilever, which may be derived from force and moment balance arguments applied to an infinitesimal element of deflected cantilever, are

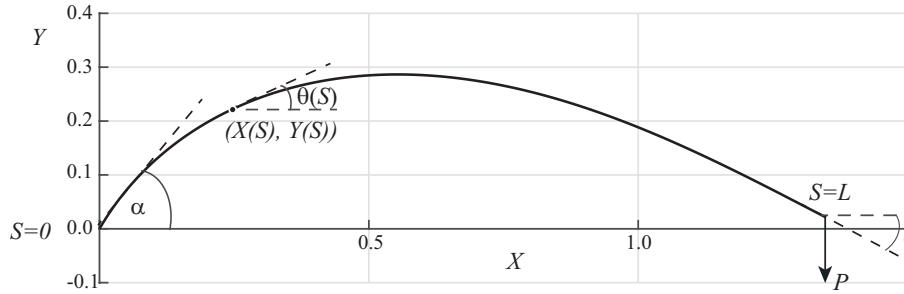


FIG. 1. A general equilibrium configuration of the deflected cantilever inclined at angle α under an end load P with reference to the (X, Y) coordinate frame.

$$(2.1) \quad \frac{d^2\theta}{dS^2} = \frac{P}{EI} \cos(\theta),$$

$$(2.2) \quad \frac{dX}{dS} = \cos(\theta),$$

$$(2.3) \quad \frac{dY}{dS} = \sin(\theta).$$

where EI is the flexural rigidity of the cantilever. The boundary conditions are

$$(2.4) \quad \theta(0) = \alpha,$$

$$(2.5) \quad \frac{d\theta(L)}{dS} = 0,$$

$$(2.6) \quad X(0) = 0,$$

$$(2.7) \quad Y(0) = 0.$$

We are interested in solutions for equilibrium configurations for which $X(L) \geq 0$ and in particular $X(L)$ a maximum for a given load P . In that case we may confine ourselves to values of α given by

$$(2.8) \quad -\frac{\pi}{2} \leq \alpha < \frac{3\pi}{2}.$$

Furthermore, when $\alpha > \pi/2$, the angle at the free end or tip $\gamma = \theta(L)$ is restricted by

$$(2.9) \quad \gamma \leq -\alpha + \pi.$$

That is because for those values of α , we are deflecting the cantilever against the natural direction of deflection. It is a relatively simple procedure to obtain the exact solutions to Eqs. (2.1)–(2.3) subject to the boundary conditions given

by Eqs. (2.4)–(2.7), see Frisch-Fay [13] or Dym [14]. We just state them as follows

$$(2.10) \quad S = \left(\frac{EI}{P}\right)^{\frac{1}{2}} (F(\phi, k) - F(\phi_\alpha, k)),$$

$$(2.11) \quad X = 2\left(\frac{EI}{P}\right)^{\frac{1}{2}} k(\cos(\phi) - \cos(\phi_\alpha)),$$

$$(2.12) \quad Y = \left(\frac{EI}{P}\right)^{\frac{1}{2}} (2E(\phi, k) - F(\phi, k) - 2E(\phi_\alpha, k) + F(\phi_\alpha, k)),$$

where the elliptic modulus k and elliptic argument ϕ are defined by

$$(2.13) \quad k = \sin\left(\frac{\gamma - \pi/2}{2}\right),$$

$$(2.14) \quad \phi = \arcsin\left(\frac{\sin(\frac{\theta - \pi/2}{2})}{k}\right),$$

and ϕ_α is just the value of ϕ at $\theta = \alpha$. At $S = L$, Eqs. (2.10)–(2.12) become

$$(2.15) \quad L = \left(\frac{EI}{P}\right)^{\frac{1}{2}} (-F(\phi_\alpha, k) + K(k)),$$

$$(2.16) \quad R = -2\left(\frac{EI}{P}\right)^{\frac{1}{2}} k \cos(\phi_\alpha) = 2\left(\frac{EI}{P}\right)^{\frac{1}{2}} \left(k^2 - \frac{1}{2} + \frac{1}{2} \sin(\alpha)\right)^{\frac{1}{2}},$$

$$(2.17) \quad \Delta = \left(\frac{EI}{P}\right)^{\frac{1}{2}} (-2E(\phi_\alpha, k) + F(\phi_\alpha, k) + 2E(k) - K(k)),$$

where we have defined $R = X(L)$ and $\Delta = Y(L)$. $K(k)$ and $E(k)$ are the complete elliptic integrals of the first and second kind, respectively. $F(\phi, k)$ and $E(\phi, k)$ are the incomplete elliptic integrals of the first and second kind, respectively. See GRADSHTEYN and RYZHIK [15] for further details on elliptic integrals.

In non-dimensional units defined by

$$(2.18) \quad s = \frac{S}{L}, \quad x = \frac{X}{L}, \quad y = \frac{Y}{L}, \quad p = \frac{PL^2}{EI}$$

with $r = R/L$ and $\delta = \Delta/L$ and using Eq. (2.18), Eqs. (2.10)–(2.12) become

$$(2.19) \quad s = \frac{1}{p^{\frac{1}{2}}} (F(\phi, k) - F(\phi_\alpha, k)),$$

$$(2.20) \quad x = \frac{2k}{p^{\frac{1}{2}}} (\cos(\phi) - \cos(\phi_\alpha)),$$

$$(2.21) \quad y = \frac{1}{p^{\frac{1}{2}}} (2E(\phi, k) - F(\phi, k) - 2E(\phi_\alpha, k) + F(\phi_\alpha, k)),$$

and Eqs. (2.15)–(2.17) become

$$(2.22) \quad 1 = \frac{1}{p^{\frac{1}{2}}}(-F(\phi_\alpha, k) + K(k)),$$

$$(2.23) \quad r = -\frac{2k}{p^{\frac{1}{2}}} \cos(\phi_\alpha) = \frac{2}{p^{\frac{1}{2}}} \left(k^2 - \frac{1}{2} + \frac{1}{2} \sin(\alpha) \right)^{\frac{1}{2}},$$

$$(2.24) \quad \delta = \frac{1}{p^{\frac{1}{2}}}(-2E(\phi_\alpha, k) + F(\phi_\alpha, k) + 2E(k) - K(k)).$$

3. The snap-back instability

As reported by ARMANINI *et al.*, when the tip load p exceeds the critical load $p_c = \pi^2/4$, the quasi-statically rotated cantilever will encounter a snap-back instability [9]. That snap-back instability occurs at $\alpha = \alpha_s$, where the snap-back angle α_s depends on p . On an α – k plot, that snap-back instability manifests at the critical point (α_s, k_s) , where $k_s = k(\alpha_s)$, as shown in Fig.2. Therefore, we can determine α_s from

$$(3.1) \quad \frac{d\alpha}{dk} = 0.$$

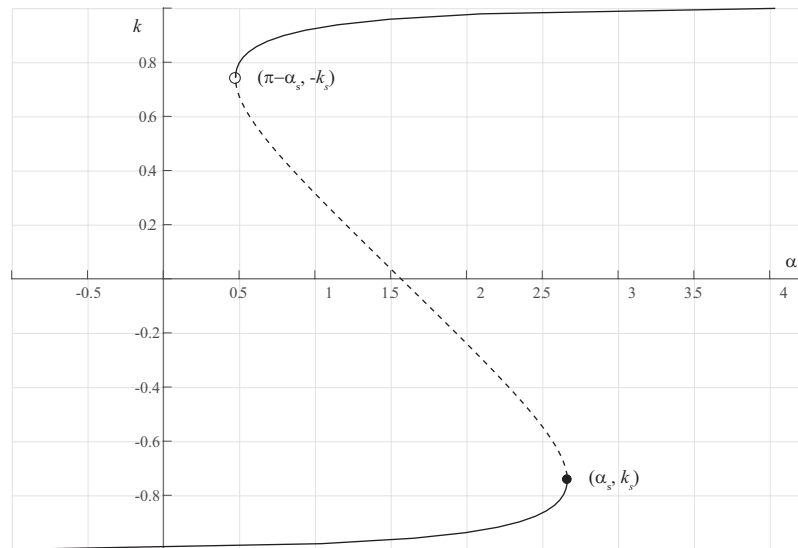


FIG. 2. A typical α – k plot for $p > p_c$ with critical points at (α_s, k_s) and $(\pi - \alpha_s, -k_s)$. In this plot, $p = 3p_c$. Stable and unstable equilibrium configurations correspond to solid and dashed parts of the curve, respectively.

From Eqs. (2.22) and (3.1), we obtain the following necessary, but not sufficient, condition for locating α_s in $-1 < k \leq 0$

$$(3.2) \quad \cos(\alpha) - 2 \left(k^2 - \sin^2 \left(\frac{\alpha - \pi/2}{2} \right) \right)^{\frac{1}{2}} \\ \times (E(\phi_\alpha, k) - E(k) - (1 - k^2)(F(\phi_\alpha, k) - K(k))) = 0.$$

Now solve Eqs. (2.22) and (3.2) simultaneously to obtain $\alpha = \alpha_s$ and $k = k_s$. We restrict k_s to $-1 < k_s \leq 0$ since we are only interested in non-negative reach, $r \geq 0$. It may be noted that there is a second critical point on the α - k plot shown in Fig. 2. Its location, by symmetry, is $(\pi - \alpha_s, -k_s)$. That second critical point corresponds to negative reach, $r < 0$, and is therefore not considered in our analysis.

An equilibrium configuration, for $p > p_c$, with a clamp angle α obtained by quasi-statically rotating the cantilever anti-clockwise from $\alpha = -\pi/2$ will be stable to the snap-back instability, and therefore realisable in practice, if

$$(3.3) \quad \alpha \leq \alpha_s.$$

4. Maximum reach

Given a cantilever with the flexural rigidity EI and length L , what is the angle of inclination α that produces the maximum reach R of the cantilever for a given load P suspended from its tip? That reach is referred to as the ‘‘furthest reach’’ by PLAUT and VIRGIN [8]; we refer to it as the maximum reach. A similar problem has been considered by ARMANINI *et al.*, where it is referred to as the ‘‘maximum horizontal distance’’ [9]. Since the flexural rigidity EI and length L are constants, we can work with non-dimensional units without loss of generality and avoid all those factors of EI and L . The reach $R = Lr$ is a maximum R_{\max} , if the reach r is a maximum r_{\max} . That occurs when

$$(4.1) \quad \frac{dr}{d\alpha} = 0.$$

When the load $p = 0$ (and therefore load $P = 0$), it is obvious that the reach $r = \cos(\alpha)$ and Eq. (4.1) implies $\alpha = 0$ and $r_{\max} = 1$. In the case when the load $p > 0$ (and therefore load $P > 0$), we use Eqs. (2.14), (2.22), (2.23) and (4.1) to find

$$(4.2) \quad 4k^2(1 - k^2) - \cos^2(\alpha) + 2 \cos(\alpha) \left(k^2 - \frac{1}{2} + \frac{1}{2} \sin(\alpha) \right)^{\frac{1}{2}} \\ \times (E(\phi_\alpha, k) - E(k) - (1 - k^2)(F(\phi_\alpha, k) - K(k))) = 0.$$

Equation (4.2) is a necessary, but not sufficient, condition to ensure that the reach r is a maximum r_{\max} . In which case the reach R is a maximum R_{\max} . To determine r_{\max} , we need to solve Eqs. (2.22) and (4.2) simultaneously for α and k . Using those values of α and k , r_{\max} can be found from Eq. (2.23).

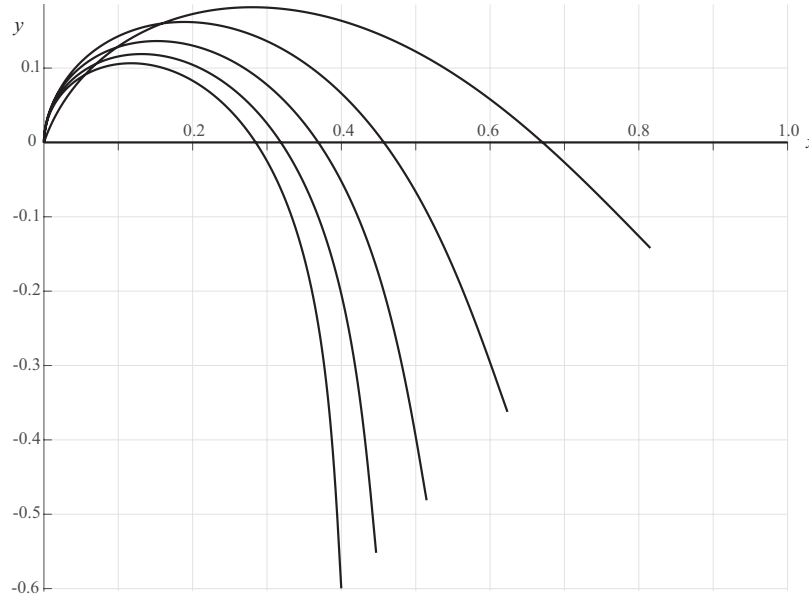


FIG. 3. Equilibrium configurations of the deflected cantilever at maximum reach, for $p = 0, 5, 10, 15, 20$ and 25 . Values of p increase as the tip of the deflected cantilever moves closer to the y -axis, or as the values of maximum reach r_{\max} decrease.

Figure 3 depicts a selection of our results for $0 \leq p \leq 25$. For $p = 0, 1, 2, 3, 4, 5$ and 6 our results are in full agreement with the experimental and numerical results of PLAUT and VIRGIN [8] including their finding for $p > 0$ that the maximum reach occurs when the tip of the cantilever is below the level of the clamped end. Our analysis is capable of producing results for loads p such that $0 \leq p < \infty$ (or loads P such that $0 \leq P < \infty$). The necessary, but not sufficient, condition for attaining maximum reach presented in Eq. (4.2) is, as far as we know, new.

PLAUT and VIRGIN [8] propose an approximation for the angle of inclination α that produces maximum reach for a given tip load p of the form

$$(4.3) \quad \alpha = 0.3484p - 0.01451p^2 - 0.001071p^3.$$

That approximation works very well for $0 \leq p \leq 6$ with a maximum error less than 0.006 radians. However, for larger values of p the error becomes unbounded.

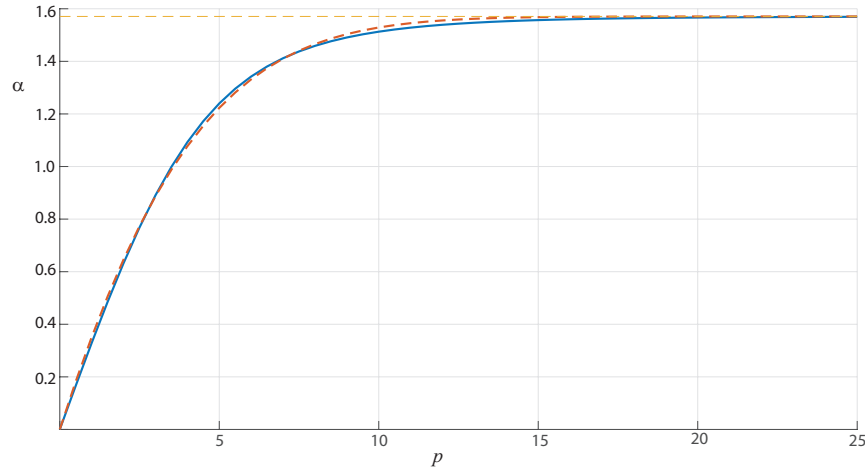


FIG. 4. Angle α for maximum reach as a function of p . The dashed line is the approximation for α given by Eqs. (4.4) and (4.5). The horizontal dashed line represents the asymptote $\alpha = \pi/2$.

Inspired by the approximation of Plaut and Virgin given by Eq. (4.3) and on inspecting Fig. 4, we notice that the numerical solution for α is characterised by $\alpha = 0$ at $p = 0$ and $\alpha \rightarrow \pi/2$ as $p \rightarrow \infty$. We therefore propose the approximation

$$(4.4) \quad \alpha = \frac{\pi}{2}(1 - e^{-(ap+bp^2+cp^3)})$$

where a , b , and c are positive constants. If we consider the numerical solution for α for $0 \leq p \leq 25$ shown in Fig. 4, we can use a suitable function fitting algorithm and obtain

$$(4.5) \quad a = 0.2409, \quad b = 0.01213, \quad c = 7.625 \times 10^{-10}.$$

The important point to bear in mind when an approximation is used is to know the maximum error over the range of values of p being considered. For $0 \leq p \leq 25$, the approximation given by Eqs (4.4) and (4.5) gives a maximum error of about -0.0222 radians, see Fig. 4. Over that same range of values for p , the maximum error for the approximation given by Eq. (4.3) is 18.6625 radians. Other valid approximations for α as a function of p can be found over other various ranges for p with some determinable maximum error. Incidentally, it must be pointed out that Fig. 4 is in complete agreement with the subpart of Fig. 9(b) presented in ARMANINI *et al.* [9].

Before investigating another maximum reach problem, we make a few remarks on the maximum reach problem just solved.

1. When $p = 0$, the cantilever is undeflected, the angle of inclination $\alpha = 0$ and the maximum reach $r_{\max} = 1$.
2. For a given load p such that $0 < p < \infty$, the maximum reach r_{\max} is attained for some angle of inclination α such that $0 < \alpha < \pi/2$, where p and α satisfy Eqs. (2.22) and (4.2).
3. In $0 \leq \alpha \leq \pi/2$, the elliptic modulus $k = \sin((\alpha - \pi/2)/2)$ is a zero of Eq. (4.2).
4. In $\pi/2 < \alpha < 3\pi/2$, the elliptic modulus $k = -\sin((\alpha - \pi/2)/2)$ is a zero of Eq. (4.2). Furthermore, at that value of k , the associated value of the load p is

$$(4.6) \quad p = 4K^2 \left(\sin \left(\frac{\alpha - \pi/2}{2} \right) \right)$$

and the reach r is a minimum, $r_{\min} = 0$, see Fig. 5. As a consequence of Eqs. (2.9) and (4.6), in $\pi/2 < \alpha < 3\pi/2$, the load p is constrained by

$$(4.7) \quad p > \pi^2.$$

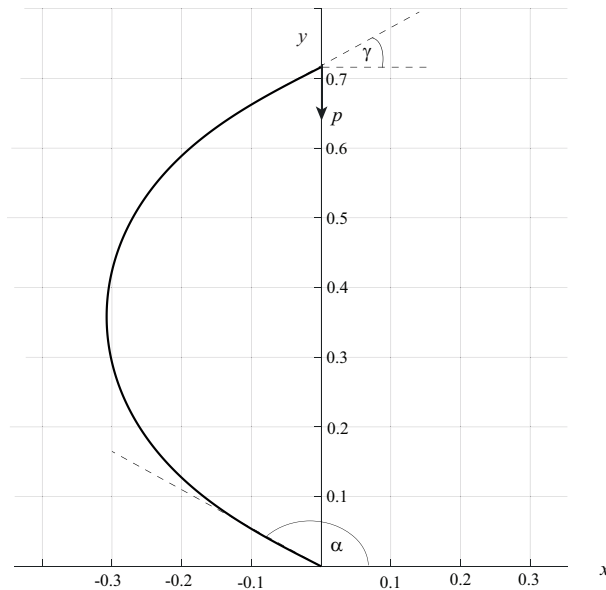


FIG. 5. A typical equilibrium configuration of a cantilever for $\pi/2 < \alpha < 3\pi/2$ with $k = -\sin((\alpha - \pi/2)/2)$, $p = 4K^2(\sin((\alpha - \pi/2)/2))$ and $r = r_{\min} = 0$.

5. Reach subject to the tip being at a given height

If a cantilever with the flexural rigidity EI and length L has to deploy a load P suspended from its tip to a height H , above or below, the level of the clamped-end, what is the angle of inclination α and the reach R of the cantilever? That question is a generalisation of the question asked by WANG [6], BATISTA [7] and ARMANINI *et al.* [9], where only the case $H = 0$ is discussed. In those papers the reach is referred to as the “longest horizontal reach”; we refer to it as the reach subject to the tip being at a given height. Obviously, the height H cannot exceed the length L of the cantilever, thus we restrict H to

$$(5.1) \quad -L < H < L.$$

The constraint on the cantilever’s free end or tip is

$$(5.2) \quad \Delta = H,$$

where Δ is given by Eq. (2.17).

As in Section 4, we can work with non-dimensional units without loss of generality and avoid all those factors of EI and L . In that case Eq. (5.1) becomes

$$(5.3) \quad -1 < h < 1$$

where $h = H/L$ and the constraint on the cantilever’s free end or tip given by Eq. (5.2) in non-dimensional form becomes

$$(5.4) \quad \delta = h,$$

where δ is given by Eq. (2.24). When the load $p = 0$ (and therefore load $P = 0$), the reach $r = \cos(\alpha)$ and Eq. (5.4) requires $\sin(\alpha) = h$. In which case $\alpha = \arcsin(h)$ and $r = (1 - h^2)^{\frac{1}{2}}$. In the case when the load $p > 0$ (and therefore load $P > 0$), we need to solve Eqs. (2.22) and (5.4) simultaneously for α and k . Using, those values of α and k , r can be found from Eq. (2.23). To be explicitly clear, for given $p > 0$ and h restricted by Eq. (5.3) we simultaneously solve

$$(5.5) \quad p^{\frac{1}{2}} + F(\phi_\alpha, k) - K(k) = 0,$$

$$(5.6) \quad (h + 1)(-F(\phi_\alpha, k) + K(k)) + 2(E(\phi_\alpha, k) - E(k)) = 0,$$

for α and k . Figures 6–8 display the equilibrium configurations of a cantilever under various loads p for a selection of values of h .

As can be see from Figs. 6–8, as the load p increases, the reach r of the cantilever decreases. In our analysis, we are only considering solutions with non-negative reach, i.e. $r \geq 0$. Thus, the least value of r is $r = 0$. That restricts p to

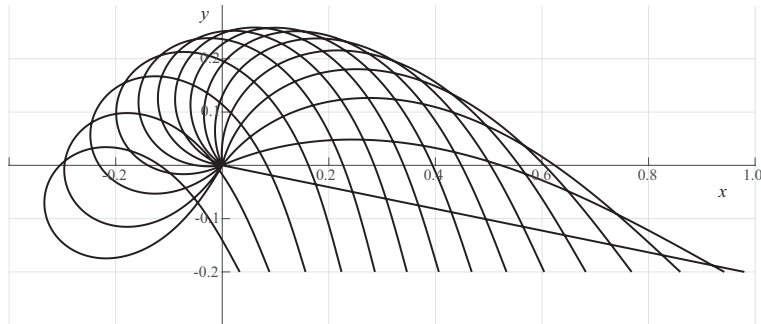


FIG. 6. Equilibrium configurations of a cantilever for $h = -0.2$ and $p = 0, 2, 4, \dots, 28$. Values of p increase as the tip of the deflected cantilever moves closer to the y -axis, or as the values of reach r decrease.

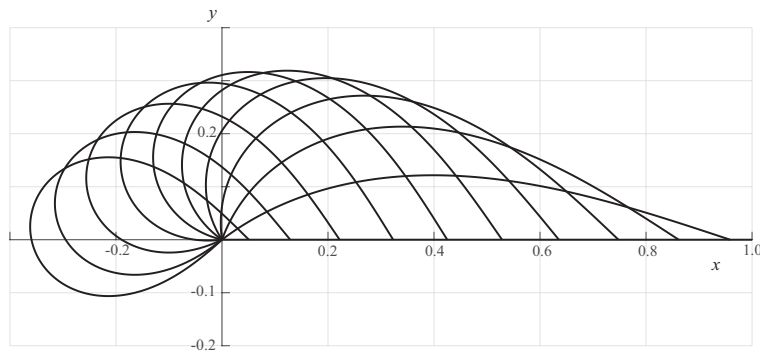


FIG. 7. Equilibrium configurations of a cantilever for $h = 0$ and $p = 0, 2, 4, \dots, 20$. Values of p increase as the tip of the deflected cantilever moves closer to the y -axis, or as the values of reach r decrease.

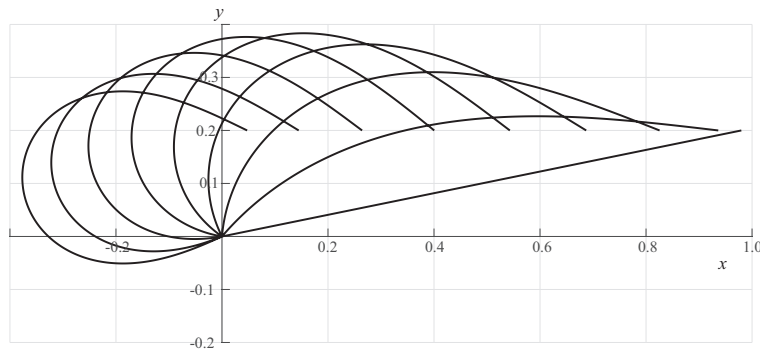


FIG. 8. Equilibrium configurations of a cantilever for $h = 0.2$ and $p = 0, 2, 4, \dots, 16$. Values of p increase as the tip of the deflected cantilever moves closer to the y -axis, or as the values of reach r decrease.

a maximal value p_m and α to some value α_m , which are determined as follows. Setting $r = 0$ in Eq. (2.23) gives

$$(5.7) \quad k = -\sin\left(\frac{\alpha - \pi/2}{2}\right).$$

Note, we have taken the solution for k with the negative sign since the positive sign corresponds to k for the undeflected cantilever. For the value of k given by Eq. (5.7), Eqs. (5.5) and (5.6) become

$$(5.8) \quad p^{\frac{1}{2}} - 2K(k) = 0,$$

$$(5.9) \quad (h + 1)K(k) - 2E(k) = 0,$$

respectively. Now solve Eq. (5.9) for k . Substitute that value of k into Eqs. (5.7) and (5.8) to obtain $\alpha = \alpha_m$ and $p = p_m$, respectively. Results obtained for a selection of values for h are presented in Table 1, where α_{m_s} is the snap-back angle for the maximal tip load p_m . For $h = 0$, the values of p_m and α_m presented in Table 1 agree with those found by BATISTA [7].

Table 1. For each value of h , the corresponding values for p_m , α_m and α_{m_s} are shown.

h	p_m	α_m	α_{m_s}
-0.2	29.3826	4.1552	4.2343
-0.1	24.8240	4.0038	4.1114
0	21.5491	3.8521	3.9928
0.1	19.0875	3.7004	3.8794
0.2	17.1700	3.5479	3.7714

Observe that $\alpha_m < \alpha_{m_s}$ in all cases in Table 1, indicating stable equilibrium configurations by Eq. (3.3). Furthermore, the values for α_{m_s} in Table 1 agree with those reported by ARMANINI *et al.*, taking into account different conventions for defining the clamp angle α and positive directions of quasi-static rotation [9].

6. Maximising the reach subject to the tip being at a given height

The load p is given in terms of the load P , length L and flexural rigidity EI of the cantilever by Eq. (2.18). If L and EI remain constants, p increases as P increases. In Figs. 6–8 we see that when p becomes sufficiently large, the cantilever is highly deflected and the reach r becomes relatively short. Since the reach $R = Lr$, this too becomes relatively short.

In order to increase the reach R of the cantilever while deploying the same load P to the same height H , we can, as proposed by WANG [6], shorten the

length L of the cantilever to achieve this. We clarify, that it must be the physical cantilever that is shortened through its length L and not the non-dimensional cantilever whose length is always normalised to one.

Suppose the length L of the cantilever is shortened by some factor $\lambda < 1$ and becomes L_* where

$$(6.1) \quad L_* = \lambda L.$$

Then, for the same load P , the loads p and p_* associated with the cantilever lengths L and L_* , respectively, are related by

$$(6.2) \quad p_* = \lambda^2 p.$$

The fully dimensional physical equations describing the equilibrium configurations of the cantilever of shortened length L_* are easily obtained from Eqs. (2.8)–(2.17) by replacing $\alpha, k, \gamma, S, X, Y, L, R$, and Δ with $\alpha_*, k_*, \gamma_*, S_*, X_*, Y_*, L_*, R_*$, and Δ_* , respectively. Note that the flexural rigidity EI and H , as well as P , all remain constant.

We use λ to vary L_* in Eq. (6.1) in order to maximise the reach R_* subject to the constraint

$$(6.3) \quad \Delta_* = H,$$

for the same load P . We point out that we use the same height H for the shortened cantilever of length L_* as we did for the original cantilever of length L . That is to ensure that we deploy the same load P to the same height H for both cantilevers. Therefore, H must satisfy

$$(6.4) \quad -L < L_* < H < L_* < L.$$

Or, equivalently h must satisfy

$$(6.5) \quad -1 < -\lambda < h < \lambda < 1,$$

where $h = H/L$. Equations (6.4) and (6.5) imply that there are limits on H and h and therefore care must be exercised when choosing them.

The condition for maximising the reach R_* of the cantilever by varying λ is

$$(6.6) \quad \frac{dR_*}{d\lambda} = 0.$$

Using Eqs. (2.14), (2.16), (2.17), (6.3) and (6.6), with quantities appropriately subscripted with $*$, we find

$$(6.7) \quad (2k_*^2 - 1) \cos^2(\alpha_*) + 4k_*^2(1 - k_*^2) \sin(\alpha_*) \\ - 2 \cos(\alpha_*) \left(k_*^2 - \frac{1}{2} + \frac{1}{2} \sin(\alpha_*) \right)^{\frac{1}{2}} \\ \times ((2k_*^2 - 1)(E(\phi_{\alpha_*}, k_*) - E(k_*)) + (1 - k_*^2)(F(\phi_{\alpha_*}, k_*) - K(k_*))) = 0.$$

Equation (6.7) is a necessary, but not sufficient, condition to ensure that the reach R_* is a maximum. As far as we know it is new, although BATISTA [7] has a version in terms of Jacobi elliptic functions derived for $H = 0$ (or $h = 0$). ARMANINI *et al.* also discuss shortening the physical length to maximise the physical reach [9]. However, they do not give any condition of the form in Eq. (6.7) explicitly. From Eqs. (2.17) and (6.3) we have

$$(6.8) \quad hp^{\frac{1}{2}} + 2(E(\phi_{\alpha_*}, k_*) - E(k_*)) - F(\phi_{\alpha_*}, k_*) + K(k_*) = 0$$

and from Eqs. (2.15) and (2.18) (or alternatively Eq. (2.22)) we obtain

$$(6.9) \quad p_*^{\frac{1}{2}} = -F(\phi_{\alpha_*}, k_*) + K(k_*).$$

We determine α_* and k_* by simultaneously solving Eqs. (6.7) and (6.8) for given p and h . Then, substitute those values of α_* and k_* into Eq. (6.9) to obtain p_* . Once p_* , α_* and k_* are known, the equilibrium configuration representing the maximised reach R_* is fully determined. The value of λ is found from Eq. (6.2) and therefore L_* can then be determined from Eq. (6.1).

A simple calculation gives the following important ratio

$$(6.10) \quad \frac{R_*}{R} = \lambda \frac{r_*}{r} = \frac{(k_*^2 - \frac{1}{2} + \frac{1}{2} \sin(\alpha_*))^{\frac{1}{2}}}{(k^2 - \frac{1}{2} + \frac{1}{2} \sin(\alpha))^{\frac{1}{2}}},$$

where r and r_* are the non-dimensional reaches associated with the physical reaches R and R_* , respectively. Equation (6.10) allows a direct comparison of by how much the maximised reach R_* is greater than the reach R (for the same load P and height H). Specific values of L and L_* are not needed for that comparison. We only need α and k for the cantilever of length L and flexural rigidity EI deploying a load P to height H and α_* and k_* for the cantilever with maximised reach R_* , shortened length L_* and flexural rigidity EI also deploying a load P to height H .

We now present results for a selection of values for h . For each value of h a table is shown displaying values for p , α , α_s , r , p_* , α_* , α_{*s} , r_* , λ and R_*/R , where α_s and α_{*s} are the snap-back angles for tip loads p and p_* , respectively. Also, for each table of results for a given value of h , we display a figure containing two plots of the shapes of the deflected cantilever; the plot on the left is in non-dimensional units and the plot on the right is in physical (dimensional) units. For the latter, we assume some value for the length L of the cantilever in metres (m) and take the flexural rigidity $EI = 0.0034 \text{ Nm}^2$ (which incidentally corresponds to a nitinol strip of width 0.003 m and thickness 0.0005 m). In each plot, both non-dimensional and dimensional, there are two curves; the dashed

Table 2. Results for maximising the reach for $h = -0.2$.

p	α	α_s	r	p_*	α_*	α_{*s}	r_*	λ	R_*/R
10	1.9810	3.0969	0.6042	8.2834	1.6742	2.8279	0.6730	0.9101	1.0137
12	2.2570	3.3449	0.5335	8.5217	1.6657	2.8688	0.6655	0.8427	1.0513
14	2.5174	3.5395	0.4682	8.7500	1.6583	2.9069	0.6585	0.7906	1.1120
16	2.7712	3.6947	0.4065	8.9704	1.6518	2.9426	0.6518	0.7488	1.2007
18	3.0259	3.8206	0.3466	9.1845	1.6461	2.9764	0.6454	0.7143	1.3301
20	3.2896	3.9244	0.2865	9.3932	1.6410	3.0085	0.6393	0.6853	1.5291
22	3.5705	4.0110	0.2238	9.5975	1.6364	3.0390	0.6334	0.6605	1.8692
24	3.8676	4.0844	0.1563	9.7979	1.6322	3.0682	0.6278	0.6389	2.5663
26	4.1138	4.1471	0.0886	9.9948	1.6284	3.0962	0.6223	0.6200	4.3549
28	4.1891	4.2011	0.0327	10.1887	1.6249	3.1231	0.6170	0.6032	11.3679

Table 3. Results for maximising the reach for $h = 0$.

p	α	α_s	r	p_*	α_*	α_{*s}	r_*	λ	R_*/R
8	2.1408	2.7775	0.6356	6.3779	1.7976	2.4537	0.7265	0.8929	1.0205
10	2.5317	3.0969	0.5284	6.3779	1.7976	2.4537	0.7265	0.7986	1.0980
12	2.9032	3.3449	0.4250	6.3779	1.7976	2.4537	0.7265	0.7290	1.2461
14	3.2626	3.5395	0.3230	6.3779	1.7976	2.4537	0.7265	0.6750	1.5180
16	3.5906	3.6947	0.2220	6.3779	1.7976	2.4537	0.7265	0.6314	2.0661
18	3.8165	3.8206	0.1288	6.3779	1.7976	2.4537	0.7265	0.5953	3.3572
20	3.8859	3.9244	0.0509	6.3779	1.7976	2.4537	0.7265	0.5647	8.0664

curve represents the original cantilever of length L and the solid curve represents the cantilever shortened to length L_* to maximise the reach R_* .

We have shown the shapes of the deflected cantilever in physical (dimensional) units because we feel that the effect of length shortening can only be appreciated in physical units. The non-dimensional shapes of the deflected cantilever, by definition, are always of unit length and length shortening, as mentioned before makes little sense in this non-dimensional case.

When $H = 0$ (or $h = 0$),

$$(6.11) \quad p_* = 6.3779, \quad \alpha_* = 1.7976, \quad k_* = -0.9243.$$

Those values for p_* , α_* and k_* are in agreement with WANG [6] and BATISTA [7] (taking into account different sign conventions for the elliptic modulus k). Furthermore, it can be shown from Eqs. (2.23) and (6.11) that the reach $r_* = 0.7265$. Also

$$(6.12) \quad \lambda = \frac{2.5254}{p_*^{\frac{1}{2}}}$$

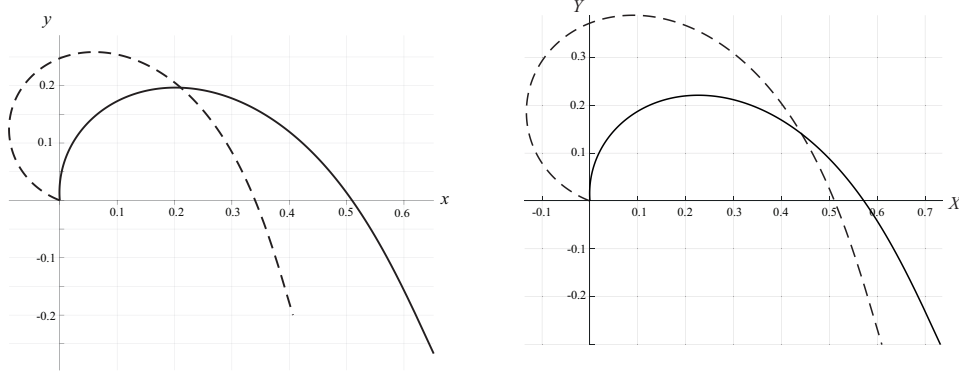


FIG. 9. Equilibrium configurations for $h = -0.2$. The plot on the left is in non-dimensional units and the plot on the right is in physical (dimensional) units. In the plot on the left, the dashed curve represents the original cantilever with $p = 16$ and the solid curve represents the shortened cantilever with $p_* = 8.9704$. In the plot on the right, where $H = -0.3$ m (equivalent to $h = -0.2$), the dashed curve represents the original cantilever with $EI = 0.0034 \text{ Nm}^2$, $L = 1.5$ m, $P = 0.0242$ N (equivalent to $p = 16$) and $R = 0.6097$ m and the solid curve represents the shortened cantilever with $EI = 0.0034 \text{ Nm}^2$, $L_* = 1.1231$ m, $P = 0.0242$ N (equivalent to $p_* = 8.9704$) and $R_* = 0.7321$ m. See the row with $p = 16$ in Table 2 for details.

Table 4. Results for maximising the reach for $h = 0.2$.

p	α	α_s	r	p_*	α_*	α_{*s}	r_*	λ	R_*/R
6	2.0384	2.3695	0.6871	5.5543	1.9318	2.2660	0.7160	0.9621	1.0025
8	2.5312	2.7775	0.5431	5.4714	1.9547	2.2463	0.7087	0.8270	1.0792
10	2.9693	3.0969	0.4004	5.4077	1.9753	2.2310	0.7009	0.7354	1.2873
12	3.3225	3.3449	0.2643	5.3576	1.9940	2.2190	0.6927	0.6682	1.7512
14	3.5295	3.5395	0.1447	5.3178	2.0114	2.2094	0.6842	0.6163	2.9139
16	3.5764	3.6947	0.0475	5.2862	2.0277	2.2018	0.6755	0.5748	8.1773

and from Eqs. (6.10) and (6.11) we have

$$(6.13) \quad \frac{R_*}{R} = \frac{0.9173}{\left(k^2 - \frac{1}{2} + \frac{1}{2} \sin(\alpha)\right)^{\frac{1}{2}}}.$$

An important fact to notice is that p_* , α_* and k_* are constants with no dependence on p . That is because the term which introduces p dependence into the system via a coupling with h , $hp^{\frac{1}{2}}$ in Eq. (6.8), vanishes when $h = 0$ (or $H = 0$).

When $H \neq 0$ (or $h \neq 0$), as demonstrated in our results, we can still maximise the reach R_* provided Eqs. (6.4) and (6.5) are respected. However, now since $h \neq 0$, the term $hp^{\frac{1}{2}}$ in Eq. (6.8) introduces a dependency on p via a coupling with h . In that case, as p changes, so do p_* , α_* and k_* as can be seen in Tables 2

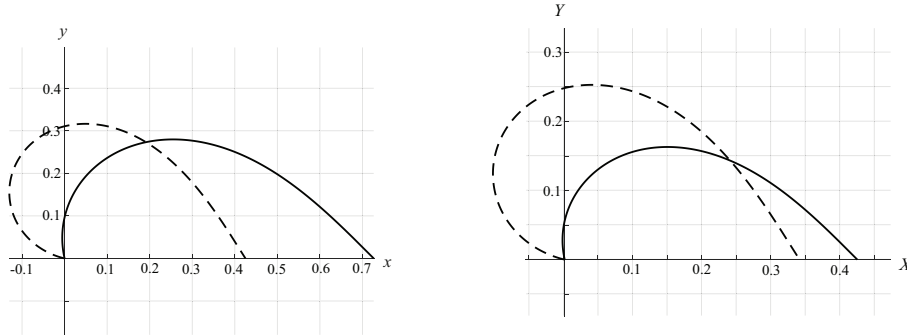


FIG. 10. Equilibrium configurations for $h = 0$. The plot on the left is in non-dimensional units and the plot on the right is in physical (dimensional) units. In the plot on the left, the dashed curve represents the original cantilever with $p = 12$ and the solid curve represents the shortened cantilever with $p_* = 6.3779$. In the plot on the right, where $H = 0$ m (equivalent to $h = 0$), the dashed curve represents the original cantilever with $EI = 0.0034 \text{ Nm}^2$, $L = 0.8$ m, $P = 0.0638$ N (equivalent to $p = 12$) and $R = 0.34$ m and the solid curve represents the shortened cantilever with $EI = 0.0034 \text{ Nm}^2$, $L_* = 0.5832$ m, $P = 0.0638$ N (equivalent to $p_* = 6.3779$) and $R_* = 0.4237$ m. See the row with $p = 12$ in Table 3 for details.

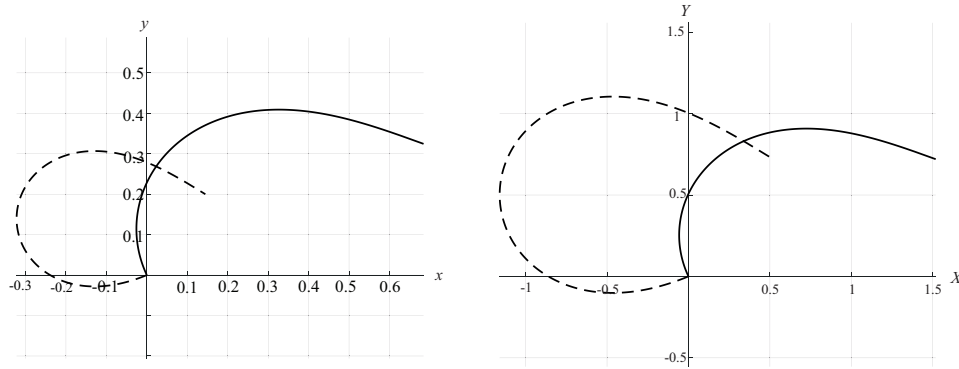


FIG. 11. Equilibrium configurations for $h = 0.2$. The plot on the left is in non-dimensional units and the plot on the right is in physical (dimensional) units. In the plot on the left, the dashed curve represents the original cantilever with $p = 14$ and the solid curve represents the shortened cantilever with $p_* = 5.3178$. In the plot on the right, where $H = 0.72$ m (equivalent to $h = 0.2$), the dashed curve represents the original cantilever with $EI = 0.0034 \text{ Nm}^2$, $L = 3.6$ m, $P = 0.0037$ N (equivalent to $p = 14$) and $R = 0.521$ m and the solid curve represents the shortened cantilever with $EI = 0.0034 \text{ Nm}^2$, $L_* = 2.2187$ m, $P = 0.0037$ N (equivalent to $p_* = 5.3178$) and $R_* = 1.5181$ m. See the row with $p = 14$ in Table 4 for details.

and 4. As a consequence of p_* , α_* and k_* not being constants, Eqs. (6.11)–(6.13) have no counterparts for $H \neq 0$ (or $h \neq 0$).

Finally, note in Tables 2–4 that $\alpha < \alpha_s$ and $\alpha_* < \alpha_{*s}$ in all cases. Therefore, from Eq. (3.3), all equilibrium configurations being considered are stable to the snap-back instability.

7. Conclusion

We have presented a necessary, but not sufficient, condition for locating the snap-back angle α_s for a given tip load p , when $p > p_c$, see Eq. (3.2). Although Armanini et al discuss the snap-back instability and the angle α_s at which it occurs in detail, they do not give a precise mathematical condition for locating α_s [9]. Furthermore, a useful test for establishing the stability of an equilibrium configuration to snap-back is given by Eq. (3.3).

The angle of the inclination α and maximum reach r_{\max} of a cantilever with a given load p suspended from its tip is determined. That problem, to some extent, is investigated by Plaut and Virgin where it is referred to as the “furthest reach” [8]. However, their investigation mainly focusses on experiments and numerical solutions and confines itself to loads p such that $0 \leq p \leq 6$. Armanini *et al.* also investigate that problem where it is referred to as the “maximum horizontal distance” [9]. Although they too concentrate on numerical solutions and experiments, they do consider loads p such that $0 \leq p < \infty$. Our analysis is valid for all loads p such that $0 \leq p < \infty$. For $0 \leq p \leq 6$, the results from our analysis are in agreement with the results of Plaut and Virgin [8], especially their finding that the maximum reach occurs when the tip is below the level of the clamped end for $p > 0$, see Fig. 3. For $0 \leq p < \infty$, our results are in agreement with Armanini et al [9]. In addition, we have presented, as far as we know, a new necessary, but not sufficient, condition for determining the maximum reach r_{\max} , see Eq. (4.2). That condition is neither in Plaut and Virgin [8] nor Armanini *et al.* [9]. Furthermore, we have given an approximation for the angle of inclination α , required to attain maximum reach r_{\max} , as a function of the load p that is valid over a greater range of values of the load p than that of Plaut and Virgin [8], see Eqs. (4.4) and (4.5). We remark that approximation is not to be found in Armanini *et al.* [9].

The problem of determining the angle of inclination α and reach r of a cantilever required to deploy a load p suspended from its tip to a height h , above or below, the clamped end is also solved. That problem is a generalisation of the “longest horizontal reach” problem investigated by WANG [6], BATISTA [7] and ARMANINI *et al.* [9], where only the case $h = 0$ is discussed.

Keeping the load P and height of load deployment H constant, we have also solved the problem of maximising the reach from R to R_* by shortening the length of the cantilever from L to L_* . That solution involved the derivation of a necessary, but not sufficient, condition for maximising R_* given by Eq. (6.7). As far as we know that condition is new, although BATISTA [7] has a version in terms of Jacobi elliptic functions derived for $H = 0$ (or $h = 0$). ARMANINI *et al.* do not give any condition of the form in Eq. (6.7) explicitly [9]. Realistic physical examples are provided that visibly demonstrate the effect of maximising

the reach by shortening the cantilever in Tables 2–4 and Figures 9–11. The importance of working in physical (dimensional) units is stressed since we believe shortening a cantilever in non-dimensional units, where the length is always normalised to one, makes no sense. Our work clarifies the process of increasing cantilever reach R by shortening its length L by emphasising the need to work in physical (dimensional) units.

In Section 4, we always consider equilibrium configurations which have $0 \leq \alpha < \pi/2$, with $\alpha \rightarrow \pi/2$ as $p \rightarrow \infty$, see Fig. 4. For $p > p_c$, we know that $\alpha_s > \pi/2$, see Fig. 2. Therefore, by Eq. (3.3), snap-back instability never occurs and maximum reach r_{\max} is always attained. However, in Sections 5 and 6, we consider equilibrium configurations for $p > p_c$ which often have $\alpha > \pi/2$. Therefore, we must consider the possibility that those equilibrium configurations could be unstable to the snap-back instability. An important observation is that all of the equilibrium configurations of the tip-loaded cantilever considered in Sections 5 and 6 are stable to the snap-back instability. That is a consequence of only considering p such that $p \leq p_m$, where p_m is the maximal load for a given h , see Table 1. For a given h , an equilibrium configuration with $p_c < p \leq p_m$ always appears to have $\alpha < \alpha_s$, in which case it is stable to the snap-back instability by Eq. (3.3). In effect, restricting p to $p \leq p_m$ for a given h ensures that the reach r is restricted to $r \geq 0$. To achieve snap-back, an unstable equilibrium configuration with $r \geq 0$ would have to snap-back to a stable equilibrium configuration with $r < 0$. Our restriction $r \geq 0$, ensured by $p \leq p_m$, effectively prevents that. Those considerations are very useful to know in load deployment situations where snap-back must be avoided.

Acknowledgements

This research was funded by London South Bank University. We would like to thank the reviewers for valuable comments and suggestions.

References

1. K.E. BISSHOPP, D.C. DRUCKER, *Large deflection of cantilever beams*, Quarterly of Applied Mathematics, **3**, 272–275, 1945.
2. C.Y. WANG, *Large deflections of an inclined cantilever with an end load*, International Journal of Non-Linear Mechanics, **16**, 2, 155–164, 1981.
3. S. NAVAEI, R.E. ELLING, *Equilibrium configurations of cantilever beams subjected to inclined end loads*, Journal of Applied Mechanics, **59**, 3, 572–579, 1992.
4. S. NAVAEI, R.E. ELLING, *Possible ranges of end slope for cantilever beams*, Journal of Engineering Mechanics, **119**, 3, 630–635, 1993.

5. M. BATISTA, *Analytical treatment of equilibrium configurations of cantilever under terminal loads using Jacobi elliptical functions*, International Journal of Solids and Structures, **51**, 13, 2308–2326, 2014.
6. C.Y. WANG, *Longest reach of a cantilever with a tip load*, European Journal of Physics, **37**, 1, 012001, 2016.
7. M. BATISTA, *Comment on ‘Longest reach of a cantilever with a tip load’*, European Journal of Physics, **37**, 5, 058004, 2016.
8. R.H. PLAUT, L.N. VIRGIN, *Furthest reach of a uniform cantilevered elastica*, Mechanics Research Communications, **83**, 18–21, 2017.
9. C. ARMANINI, F. DAL CORSO, D. MISSERONI, D. BIGONI, *From the elastica compass to the elastica catapult: an essay on the mechanics of soft robot arm*, Proceedings of the Royal Society A, **473**, 20160870, 2017.
10. M. KANEKO, N. KANAYAMA, T. TSUJI, *Active antenna for contact sensing*, IEEE Transactions on Robotics and Automation, **14**, 2, 278–291, 1998.
11. T. MICHELS, I.W. RANGELOW, *Review of scanning probe micromachining and its applications within nanoscience*, Microelectronic Engineering, **126**, 191–203, 2014.
12. G. GAO, H. WANG, Q. XIA, M. SONG, H. REN, *Study on the load capacity of a single-section continuum manipulator*, Mechanism and Machine Theory, **104**, 313–326, 2016.
13. R. FRISCH-FAY, *Flexible Bars*, Butterworths, London, pp. 33–64, 1962.
14. C.L. DYM, I.H. SHAMES, *Solid Mechanics: A Variational Approach*, augmented Edition, Springer, New York, pp. 516–521, 2013.
15. I.S. GRADSHTEYN, I.M. RYZHIK, *Table of Integrals, Series, and Products*, 7th Edition, Elsevier Academic Press, San Diego, pp. 859–883, 2007.

Received April 14, 2019; revised version September 4, 2019.

Published online December 3, 2019.
